J Therm Anal Calorim (2010) 99:531–538
DOI 10.1007/s10973-009-0113-5

# Study of kinetics and thermodynamics of the dehydration reaction of $AlPO_4 \cdot H_2O$

**Banjong Boonchom · Samart Kongtaweelert**

Published online: 23 June 2009


**Abstract** The kinetics and thermodynamics of the thermal dehydration of aluminum phosphate monohydrate, $AlPO_4 \cdot H_2O$ were studied using thermogravimetry (TG-DTG-DTA) at four heating rates in dry air atmosphere. The activation energies of the dehydration step of $AlPO_4 \cdot H_2O$ were calculated through the methods of Friedman (FR) and Flynn–Wall–Ozawa (FWO) and the possible conversion function has been estimated through the Achar and Li–Tang equations. The independent activation energies on extent of conversions and the better kinetic model of the dehydration reaction for $AlPO_4 \cdot H_2O$ indicate single kinetic mechanism and the $F_{2.05}$ model as a simple n-order reaction of "chemical process or mechanism no-invoking equation", respectively. The positive values of $\Delta H^{\#}$ and $\Delta G^{\#}$ for the dehydration reaction show that it is endothermic and non-spontaneous process and it is connected with the introduction of heat. The kinetic and thermodynamic functions calculated for the dehydration reaction by different techniques and methods were found to be consistent.

**Keywords** Aluminum phosphate · $AlPO_4 \cdot H_2O$ · Kinetics · Thermodynamics

B. Boonchom
King Mongkut's Institute of Technology Ladkrabang, Chumphon Campus, 17/1 M. 6 Pha, Thiew District, Chumphon 86160, Thailand

B. Boonchom (✉) · S. Kongtaweelert
Department of Chemistry, Faculty of Science, King Mongkut's Institute of Technology Ladkrabang, Bangkok 10520, Thailand
e-mail: kbbanjon@kmitl.ac.th

## Introduction

Aluminum phosphate hydrates are of great interest in both environmental and technological fields [1–8]. In environmental field, aluminum phosphates help remove phosphate from wastewater, while their dissociations help regulate the release of phosphate in acidic soils [1]. In technological field, aluminum phosphates are important in the area of catalytic reactions, such as dehydration, isomerization, polymerization, alkylation [2–8]. Additionally, thermal treatment of aluminum phosphate hydrates is a great synthetic potential, which relates to the role of the water of crystallization and they may turn simple compounds into advanced materials, such as ceramics, catalysts and glasses [1–5.] In this respect, amorphous $AlPO_4$ has attracted the interest of many researchers due to the realization that $AlPO_4$ is completely iso-structural with silica and exhibits parallel polymorphic transformation [4, 6, 7]. This solid was active catalyst in several organocationic reactions in which textural and acid–base properties were dependent on a number of variables such as aluminum salt, precipitating agent, or calcination temperatures [3–7]. Thus, in the last few years many works have undertaken a series of research studies on the synthesis, characterization and catalytic activity of different $AlPO_4$ [3–5, 7, 8]. Such as $AlPO_4$ had been prepared with thermal decomposition of variscite mineral ($AlPO_4 \cdot 2H_2O$) [1], synthetic $AlPO_4 \cdot 2H_2O$ [9] $AlPO_4 \cdot H_2O$-H1-4 [8] and $AlPO_4$-21 [2] and $Al_{1-x}Fe_xPO_4$ ($x = 0$) [4] precursors. By reason, the mechanism, thermodynamics and kinetics of solid-state reactions are needed in order to take advantage of this potential [1–3, 9]. Studies on thermodynamics, mechanisms and kinetics of solid-state reactions are challenging and difficult task with complexity resulting from the great variety of factors with diverse effects, e.g., reconstruction of solid state crystal

lattice, formation and growth of new crystallization nuclei, diffusion of gaseous reagents or reaction products, materials heat conductance, static or dynamic character of the environment, physical state of the reagents—dispersity, layer thickness, specific area and porosity, type, amount and distribution of the active centers on solid state surface, etc. [1–4, 8, 9]. The results obtained on these bases can be directly applied in materials science for the preparation of various metals and alloys, cements, ceramics, glasses, enamels, glazes, polymer and composite materials [4–7].

Herein, the formation of $AlPO_4$ amorphous from the thermal transformation of $AlPO_4 \cdot H_2O$ was followed using thermogravimetry-differential thermal analysis (TG-DTG-DTA), X-ray powder diffraction (XRD), scanning electron microscopy (SEM) and Fourier transform-infrared (FT-IR) spectroscopy. The non-isothermal kinetics analysis for the dehydration step of the aluminum phosphate was carried out using the isoconversional methods of Friedman (FR) [10] and Flynn–Wall–Ozawa (FWO) [11, 12]. The possible conversion functions had been estimated using Achar [13] and Li–Tang methods [14], which give the best description of the studied dehydration process and allow the calculation of reliable values of the kinetic parameters (*E* and *A*). The thermodynamic ($\Delta H^{\#}$, $\Delta G^{\#}$ and $\Delta S^{\#}$) and kinetic (*E, A,* mechanism and model) parameters of the dehydration reaction of $AlPO_4 \cdot H_2O$ have attracted the interesting of thermodynamic and kinetic scientists, which are discussed for the first time.

## Experimental

$AlPO_4 \cdot H_2O$ crystalline powder (analytical grade) was commercially obtained from Fluka Chemical Industries Co. Ltd and was used without further purification.

Thermal analysis measurements (thermogravimetry, TG; differential thermogravimetry, DTG; and differential thermal analysis, DTA) were carried out on a Pyris Diamond Perkin Elmer apparatus by increasing temperature from 303 to 1073 K with calcined $\alpha$-$Al_2O_3$ powder as the standard reference. The experiments were performed in dry air atmosphere, at heating rates of 5, 10, 15, and 20 K $min^{-1}$. The sample mass was kept about 6.0–10.0 mg in an aluminum crucible without pressing.

The structure of $AlPO_4 \cdot H_2O$ and its final decomposition products were studied by X-ray powder diffraction using X-ray diffractometer (Phillips PW3040, The Netherland) with Cu K$\alpha$ radiation ($\lambda = 0.1546$ nm). The morphology of the selected resulting samples was examined by scanning electron microscope (SEM) using LEO SEM VP1450 after gold coating. The room temperature FTIR spectra were recorded in the range of 4000–370 $cm^{-1}$ with eight scans on a Perkin-Elmer Spectrum GX FT-IR/FT-Raman spectrometer with the resolution of 4 $cm^{-1}$ using KBr pellets (KBr, Merck, spectroscopy grade).

## Results and discussion

### Thermal analysis

TG-DTG-DTA curves of the thermal decomposition of $AlPO_4 \cdot H_2O$ at heating rate of 10 K $min^{-1}$ are shown in Fig. 1. The TG curve shows a single well-defined step at temperatures below 573 K. The elimination of water is observed in 350–573 K. The corresponding observed weight loss is 12.58 % (0.98 mol $H_2O$) by mass, which agrees with to the theoretical value for $AlPO_4 \cdot H_2O$ (12.86 %, 1.00 $H_2O$). An endothermic effect on DTA curves is observed at 397 K, which corresponds to DTG peaks at 393 K, respectively. Further, a small exothermic effect at 864 K without appreciable weight loss is observed in the DTA curve, which can be ascribed to a transition phase from amorphous to crystalline form of $AlPO_4$ [4, 15] The retained mass of about 87.42% is compatible with the value expected for the formation of $AlPO_4$, which is verified by XRD and FTIR measurement (Figs. 2 and 3). The overall reaction is:

$$AlPO_4 \cdot H_2O \rightarrow AlPO_4 + H_2O \quad (1)$$

The thermal behavior of $AlPO_4 \cdot H_2O$ in this work exhibits single decomposition step and lower temperature, which are different from those of $AlPO_4 \cdot H_2O$–H4, [8]mineral and synthetic $AlPO_4 \cdot 2H_2O$, [1, 9] and $AlPO_4 \cdot 1.5H_2O$ [3]. The temperature at which theoretical mass loss is achieved, can be determined from the TG curve and considered to be the minimum temperatures needed for the calcinations

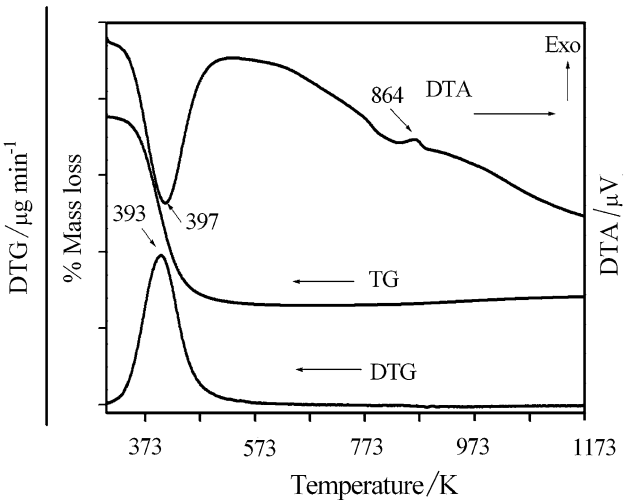


**Fig. 1** TG-DTG-DTA curves of $AlPO_4 \cdot H_2O$ in air at heating rate of 10 K $min^{-1}$

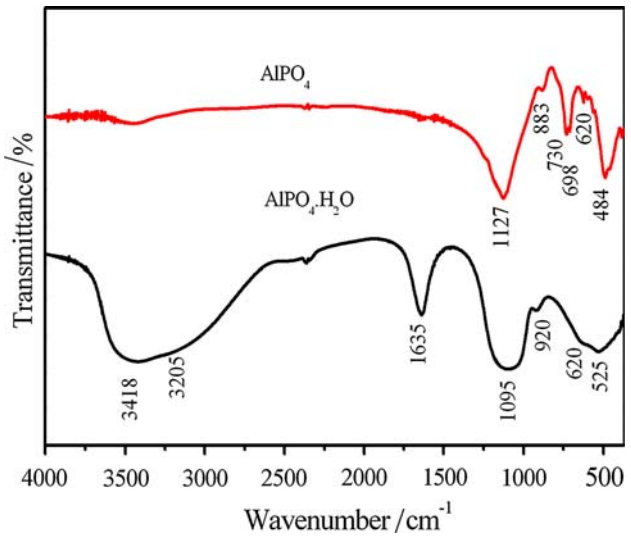


**Fig. 2** FT-IR spectra of $AlPO_4 \cdot H_2O$ (**a**) and its dehydration product ($AlPO_4$) (**b**)

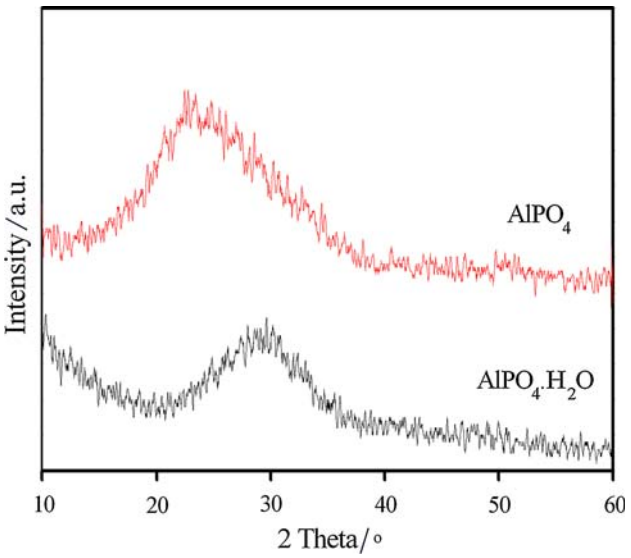


**Fig. 3** The XRD patterns of $AlPO_4 \cdot H_2O$ (**a**) and its dehydration product ($AlPO_4$) (**b**)

process. Thus, $AlPO_4 \cdot H_2O$ sample was calcined at 573 K for 2 h in the furnace, which is the lower temperature as compared to those of the other hydrate precursors [1–5]. The water in crystalline hydrate may be considered either as crystal water or as co-ordinated water. The strength of the binding of these molecules in the crystal lattice is different, hence, resulting in different dehydration temperatures. The water eliminated at 423 K and below can be considered as crystal water, whereas water eliminated at 473 and above indicates its co-ordination by the metal atom. Water molecules eliminated at intermediate temperatures can be co-ordinately linked water as well as crystal water [16]. The dehydration temperature obtained in this work suggests that the water in aluminum phosphate monohydrate can be considered as crystal water.

Following, a theoretical treatment developed by Vlase et al. [17, 18], this work apply the relation between the maximum temperature peak $T_p$ (DTA) at heating rate 10 K $min^{-1}$ and the wavenumber of activated bond is given as follows:

$$w_{sp} = \frac{k_b}{h_c} T_p = 0.695 T_p \quad (2)$$

where $k_b$ and $h$ are respectively the Boltzmann and Planck constants, and $c$ the light velocity. Because the breaking of the bond has an anharmonic behavior, the specific activation is possible also due to more than one quanta, or by a higher harmonic: $\omega_{sp} = q\omega_{calc}, q \in N = 1,2,3\ldots$, where $\omega_{sp}$ is the assigned spectroscopic wavenumber for the bond supposed to break. According to the Eq. 2, the $T_p$ (DTA) for the decomposition step is 397 K. The calculated harmonic oscillation energy ($\omega_{sp}$) values of the decomposition step were 1655, 3096 and 3554 $cm^{-1}$, which correspond to 6, 12 and 13 quanta numbers, respectively. These wavenumbers are close to the vibration of water of crystallization as reported in the literature and are assigned to symmetric bending ($\nu_2$; $A_1$), symmetric stretching ($\nu_1$; $A_1$) and asymmetric stretching ($\nu_3$; $B_2$), respectively, [19–21]. The studied compound exhibited a very good agreement between the calculated wavenumbers from average $T_p$ (DTA) and the observed wavenumbers from FT-IR spectra for the bonds suggested as being broken, which confirm thermal decomposition step corresponding to the loss of water of crystallization with different strength of hydrogen bonding. The calculated wavenumbers from average $T_p$ (DTA) using Eq. 2 are convenient and simple method for the identification of the breaking bonds during the reaction, and can be used for the discussion about the decomposition steps.

## Vibrational spectroscopy

FT-IR spectra of $AlPO_4 \cdot H_2O$ and its dehydration product ($AlPO_4$) are shown in Fig. 2. Vibrational bands are identified in relation to the crystal structure in terms of the fundamental vibrating units, namely $PO_4^{3-}$, $H_2O$, for $AlPO_4 \cdot H_2O$ and $PO_4^{3-}$ for $AlPO_4$ [19–21]. FTIR spectra of $PO_4^{3-}$ in $AlPO_4 \cdot H_2O$ and $AlPO_4$ show the antisymmetric stretching mode ($\nu_3$) in 1000–1200 $cm^{-1}$ region and the $\nu_4$ mode in 400–560 $cm^{-1}$ region. The observed bands in 1600–1700 and 3000–3500 $cm^{-1}$ region are attributed to the water bending and stretching vibrations, respectively [21] These water bands disappear in FT-IR spectra of its dehydration product ($AlPO_4$), which are in good agreement with the thermal analysis results. The XRD data along with FTIR spectra confirm that the calcined $AlPO_4 \cdot H_2O$ at 573 K for 2 h transforms to $AlPO_4$.

X-ray powder diffraction

The XRD patterns of aluminum phosphate $AlPO_4 \cdot H_2O$ and its dehydration product ($AlPO_4$) are shown in Fig. 3. The problem here is that the XRD patterns show a very low degree of crystallinity. The complexity of the spectrum makes assignment difficult. The observed broad peaks in XRD patterns indicate that poor crystallization or amorphous phase as well as namoparticles of these materials. This result is in good agreement with the results reported by Youssif et al [4] where the $AlPO_4$ transforms from amorphous to a crystalline phase at >773 K. It evidenced that this studied compound is a very stable inorganic framework system [3–5]. Additionally, the result is consistent with a transition phase from amorphous to crystalline, which is concluded in thermal analysis (864 K in DTA curve).

Scanning electron microscopy

The SEM micrographs of $AlPO_4 \cdot H_2O$ and its final decomposition product $FePO_4$ are shown in Fig. 4. The particle shape and size are changed throughout the whole decomposition product. The SEM micrograph of $AlPO_4 \cdot H_2O$ (Fig. 4a) illustrates many spherical nanoparticles of different sizes in the range of 80–200 nm The SEM micrograph of $AlPO_4$ (Fig. 4b) shows coalescence in aggregates of spherical nanoparticles of different sizes in the range of 30–100 nm. The morphology of $AlPO_4$ shows smaller size than that of $AlPO_4 \cdot H_2O$, which is the effect of the thermal dehydration process.

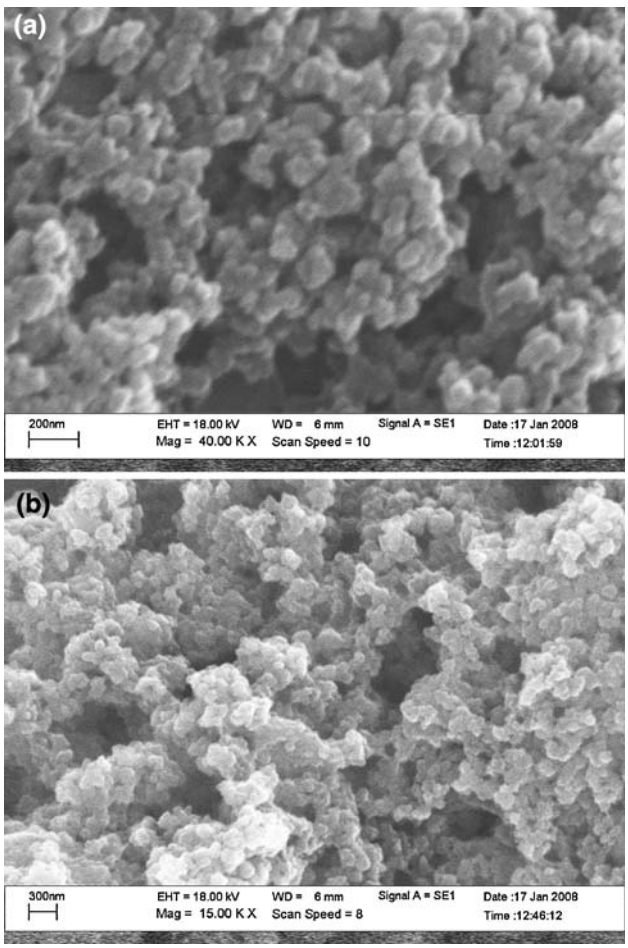


**Fig. 4** SEM micrographs of $AlPO_4 \cdot H_2O$ (**a**) and its dehydration product ($AlPO_4$) (**b**)

Kinetic and thermodynamic studies

The aim of the kinetic studies of TA data is to find the most probable kinetics model which gives the description of the studied decomposition process and allows the calculation of reliable values for the kinetic triplet ($E_a$, $A$ and reaction model). In the present work, the model-free and model fitting approaches were used to investigate the kinetics parameters under multiple-scan non-isothermal conditions, which are described as follow.

*Calculation of the activation energy by isoconversional method*

Thermal transformation of crystal hydrates is a solid-state process of the type [22–28]: A(solid) → B (solid) + C (gas). The kinetics of such reactions is described by various equations taking into account the special features of their mechanisms. The reaction can be expressed through the temperatures corresponding to fixed values of the extent of conversion ($\alpha = (m_i - m_t)/(m_t - m_f)$, where $m_i$, $m_t$ and $m_f$ are the initial, current and final sample mass, at moment time t) from experiments at different heating rates ($\beta$). To calculate the values of the activation energies ($E_\alpha$) of thermal dehydration of $AlPO_4 \cdot H_2O$, in this paper we used only the linear isoconversional methods of Friedman (FR) [10] and Flynn–Wall–Ozawa (FWO) [11, 12]

The equations used for $E_\alpha$ calculation are: Friedman (FR) equation:

$$\ln\left(\frac{d\alpha}{dt}\right) \equiv \ln\left(\beta\frac{d\alpha}{dT}\right) = \ln(Af(\alpha)) - \left(\frac{E_\alpha}{RT}\right) \quad (3)$$

Flynn–Wall–Ozawa (FWO) equation:

$$\ln\beta = \ln\left(\frac{AE_\alpha}{Rg(\alpha)}\right) - 5.331 - 1.052\left(\frac{E_\alpha}{RT}\right) \quad (4)$$

where A (the pre-exponential factor) and E (the activation energy) are the Arrhenius parameters and R is the gas constant (8.314 J $mol^{-1}$ $K^{-1}$). The Arrhenius parameters, together with the reaction model, are sometimes called the kinetic triplet. $g(\alpha) = \int_0^\alpha \frac{d\alpha}{f(\alpha)}$ is the integral form of the

reciprocal $f(\alpha)$, which is the reaction model that depends on the reaction mechanism.

According to linear isoconversional method, the basic data of $\alpha$ and $T$ collected from the TG curves of the dehydration reaction of $AlPO_4 \cdot H_2O$ at various heating rates (5, 10, 15 and 20 K $min^{-1}$) are illustrated in Table 1. According to the Eqs. 3 and 4, the plots of ln $\beta d\alpha/dT$ versus 1000/T (FR) and ln $\beta$ versus 1000/T (FWO) corresponding to different conversions $\alpha$ can be obtained by a linear regression of least-square method, respectively. The activation energies $E_\alpha$ can be calculated from the slopes of the straight lines with better linear correlation coefficient ($r^2$). The activation energies are calculated at heating rates of 5, 10, 15, and 20 K $min^{-1}$ via the FR and FWO methods in the $\alpha$ range of 0.2–0.8. The activation energies calculated by FR and FWO methods are close to each other, which are shown in Table 2, so the results are credible. The activation energy values calculated by the FR method are close to those obtained by FWO method. If $E_\alpha$ values independent on $\alpha$, the decomposition may be a simple reaction [22, 23], while the dependence of $E_\alpha$ on $\alpha$ should be interpreted in terms of multi-step reaction mechanisms [22–29]

**Table 1** $\alpha$-T data at different heating rates, $\beta$ (K$min^{-1}$), for dehydration of $AlPO_4 \cdot H_2O$

| $\alpha$ | Temperature/K | | | |
|---|---|---|---|---|
| | $\beta = 5$ | $\beta = 10$ | $\beta = 1\,5$ | $\beta = 20$ |
| 0.2 | 365.11 | 373.18 | 378.71 | 383.10 |
| 0.3 | 371.20 | 379.81 | 386.59 | 389.72 |
| 0.4 | 377.04 | 386.17 | 393.05 | 397.47 |
| 0.5 | 382.78 | 392.53 | 399.76 | 403.48 |
| 0.6 | 389.14 | 399.13 | 407.53 | 410.78 |
| 0.7 | 396.62 | 406.55 | 415.65 | 419.49 |
| 0.8 | 406.57 | 415.85 | 425.72 | 430.81 |

**Table 2** Activation energies ($E_\alpha$) versus correlation coefficient ($r^2$) calculated by FR and FWO methods for the dehydration of $AlPO_4 \cdot H_2O$

| $\alpha$ | FR method | | FWO method | |
|---|---|---|---|---|
| | $E_\alpha$/kJ $mol^{-1}$ | $r^2$ | $E_\alpha$/kJ $mol^{-1}$ | $r^2$ |
| 0.2 | 80.38 | 0.9904 | 85.53 | 0.9979 |
| 0.3 | 72.84 | 0.9961 | 83.57 | 0.9963 |
| 0.4 | 79.14 | 0.9956 | 79.82 | 0.9979 |
| 0.5 | 73.29 | 0.9899 | 80.34 | 0.9978 |
| 0.6 | 73.40 | 0.9926 | 78.23 | 0.9935 |
| 0.7 | 74.43 | 0.9858 | 77.19 | 0.9923 |
| 0.8 | 79.93 | 0.9755 | 76.87 | 0.9860 |
| Average | 76.20 ± 3.43 | 0.9894 | 80.22 ± 3.27 | 0.9940 |

Neglecting the dependence of $E$ vs $\alpha$, an average values of $E_\alpha = 81.25 \pm 4.05$ kJ $mol^{-1}$ (FR) and 79.01 ± 4.83 kJ $mol^{-1}$ (FWO) are obtained. The average activation energy of dehydration reaction of studied compound is higher and lower than those of the mineral and the synthetic $AlPO_4 \cdot 2H_2O$ (32.6 kJ $mol^{-1}$ estimated from the Freeman-Carroll method and 69.68 kJ $mol^{-1}$ from the Kissinger method) and $AlPO_4 \cdot H_2O$–H1 (130 kJ $mol^{-1}$ estimated from the Ozawa and the Kissinger–Akahira–Sonose methods), respectively. For the dehydration reaction of $AlPO_4 \cdot H_2O$, the values of activation energies change little with $\alpha$, so this process could be a single kinetic mechanism. This result is consistent with an endothermic peak at 397 K in DTA curve.

*Determination of the most probably mechanism*

The following equation were used to estimate the most correct mechanism, i.e., $g(\alpha)$ and $f(\alpha)$ functions. For dehydration reaction of $AlPO_4 \cdot H_2O$, the estimation of kinetic triplet parameters ($E_\alpha$, $A$ and kinetic function) can be turned into a multiple linear regression problem through the Achar [13] and Li–Tang equations [14].

Achar equation:

$$\ln\left(\frac{1}{f(\alpha)}\frac{d\alpha}{dT}\right) = \ln\left(\frac{AE_\alpha}{R\,g(\alpha)}\right) - \left(\frac{E_\alpha}{RT}\right) \quad (5)$$

Li–Tang equation:

$$\ln\left(\frac{g(\alpha)}{T^{1.894661}}\right) = \left[\ln\left(\frac{AE_\alpha}{\beta R}\right) + 3.63504095 - 1.894661\ln E_\alpha\right] - \left(1.0014533\frac{E_\alpha}{RT}\right) \quad (6)$$

Hence, $\ln\left(\frac{g(\alpha)}{T^{1.894661}}\right)$ and $\ln\left(\frac{1}{f(\alpha)}\frac{d\alpha}{dT}\right)$ calculated for the different $\alpha$ values at the single $\beta$ value on $1/T$ must give rise to a single master straight line, so the activation energy and the pre-exponential factor can be calculated from the slope and intercept through ordinary least square estimation. The activation energy, pre-exponential factor and the correlation coefficient can be calculated from the equations of the Achar and the Li–Tang combined with 35 conversion functions [17, 18, 22–29] Comparing the kinetic parameters from the Achar and the Li–Tang equations, the probable kinetic model may be selected, which the values of $E_\alpha$ and $A$ were calculated with the better linear correlation coefficient and the activation energies obtained from the Achar and the Li–Tang equations above were shown in good agreement to those obtained from FR and FWO methods with a better correlation coefficient ($r^2$). So the pre-exponential factor $A$ can be obtained by calculating the average value of $A(s^{-1})$ from Eqs. 5 and 6 for different heating rates.

The optimized values from the Achar and Li–Tang methods are the data of activation energy and pre-exponential factor, those were calculated with the best equation and are shown in Table 3. According to Table 3, it was seen that the values calculated by FR and FWO methods were close to the optimized values from the Achar and Li–Tang methods, and the respective correlation coefficients are preferable. This was considered enough to conclude that the kinetic parameters of non-isothermal dehydration of $AlPO_4 \cdot H_2O$ can be reliably calculated with correctly chosen $g(\alpha)$ and $f(\alpha)$ functions. Therefore, we can draw a conclusion that the obtained possible conversion function is $F_{n=2.05}$ (mechanism non-invoking equations) model for the dehydration of $AlPO_4 \cdot H_2O$, and the corresponding function is $f(\alpha) = (1 - \alpha)^{2.05}$ and $g(\alpha) = -[1 - (1 - \alpha)^{-1.05}/(1.05)$. The calculated kinetic parameters of $E_\alpha = 79.29 \pm 3.09$ kJmol$^{-1}$ (Achar) and $75.54 \pm 2.33$ kJmol$^{-1}$ (Li–Tang), $A = 1.39 \times 10^8$ s$^{-1}$ (Achar) and $5.91 \times 10^6$ s$^{-1}$ (Li–Tang), respectively. The better kinetic model of dehydration reaction of studied compound is different form that of $AlPO_4 \cdot H_2O$–H1 ($F_{2.75}$ for the Coats-Redfern and the Achar methods). Based on the values of activation energy and pre-exponential factor, the strengths of binding of water molecules in the crystal lattice are different and, hence, results in different dehydration temperatures and kinetic parameters. The activation energy for the losing of crystal water lie in the range of 60–80 kJ mol$^{-1}$, while the value for coordinately bounded one are within the range of 130–160 kJ mol$^{-1}$ [23–29]. The energy of activation found in $F_{2.05}$ model for the dehydration reaction (Table 3) suggests that the water molecules are coordinately linked water as well as crystal one. The pre-exponential factor (*A)* values in Arrhenius equation for solid phase reactions are expected to be in a wide range (six or seven orders of magnitude), even after the effect of surface area is taken into account [30–33] The low factors will often indicate a surface reaction, but if the reactions are not dependent on surface area, the low factor may indicate a "tight" complex. The high factors will usually indicate a "loose" complex. Even higher factors (after correction for surface area) can be obtained for complexes having free translation on the surface. Since the concentrations in solids are not controllable in many cases, it would have been convenient if the magnitude of the pre-exponential factor indicated for reaction molecularity. Based on these reasons, the dehydration reaction of $AlPO_4 \cdot H_2O$ may be interpreted as "loose complex", which appears to be true only for non-surface controlled reactions having low ($<10^9$ s$^{-1}$) pre-exponential factor [30–33] These results are consistent with thermal analysis, which confirm that the decomposition product is aluminum phosphate ($AlPO_4$).

**Table 3** Values of kinetic (*E, A, n*) and thermodynamic ($\Delta S^{\#}$, $\Delta H^{\#}$ *and* $\Delta G^{\#}$) functions for dehydration reaction of $AlPO_{24} \cdot H_2O$ obtained from the differential method and integral method at different heating rates ($\beta = 5$, 10,15, 20 K min$^{-1}$)

| β/ Kmin$^{-1}$ | Tp/K (DTA) | Model Fn | Achar method | | | | | | Li-Tang method | | | | | |
|---|---|---|---|---|---|---|---|---|---|---|---|---|---|---|
| | | | $E_\alpha$/kJ mol$^{-1}$ | $A$/s$^{-1}$ | $\Delta S^{\#}$/J(molK)$^{-1}$ | $\Delta G^{\#}$/kJmol$^{-1}$ | $\Delta H^{\#}$/ kJmol$^{-1}$ | $r^2$ | Eα/kJ mol$^{-1}$ | $A$/s$^{-1}$ | $\Delta S^{\#}$/J(molK)$^{-1}$ | $\Delta G^{\#}$/kJmol$^{-1}$ | $\Delta H^{\#}$/ kJmol$^{-1}$ | $r^2$ |
| 5 | 381.81 | $F_{2.05}$ | 75.58 | $4.49 \times 10^8$ | −89.64 | 106.63 | 72.41 | 0.9971 | 77.13 | $1.32 \times 10^7$ | −118.97 | 119.38 | 73.96 | 0.9966 |
| 10 | 397.41 | $F_{2.05}$ | 83.08 | $2.87 \times 10^8$ | −93.70 | 117.01 | 79.78 | 0.9948 | 77.91 | $9.08 \times 10^6$ | −122.41 | 123.25 | 74.61 | 0.9991 |
| 15 | 405.71 | $F_{2.05}$ | 78.78 | $5.23 \times 10^7$ | −108.02 | 119.23 | 75.41 | 0.9933 | 73.25 | $1.37 \times 10^6$ | −138.31 | 125.99 | 69.88 | 0.9991 |
| 20 | 410.52 | $F_{2.05}$ | 79.71 | $5.46 \times 10^7$ | −107.76 | 120.54 | 76.30 | 0.9979 | 73.86 | $1.30 \times 10^6$ | −138.84 | 127.44 | 70.45 | 0.9971 |
| Av. | 398.86 | $F_{2.05}$ | 79.29 ± 3.09 | $2.11 \times 10^8$ ± $1.93 \times 10^8$ | −99.78 ± 9.51 | 115.85 ± 6.32 | 75.97 ± 3.03 | 0.9958 | 75.54 ± 2.33 | $6.24 \times 10^6$ ± $5.91 \times 10^6$ | −129.63 ± 10.42 | 124.02 ± 3.55 | 72.22 ± 2.40 | 0.9980 |

*Av.* Average

*Determination of the thermodynamic activation parameters*

From the activated complex theory (transition state) of Eyring [30–33], the following general equation may be written:

$$A = \left(\frac{e\chi k_B T_p}{h}\right) \exp\left(\frac{\Delta S^{\#}}{R}\right) \quad (7)$$

where $A$ is the average activation energy $A$ of the Achar and the Li–Tang methods (Table 3), $e = 2.7183$ is the Neper number; $\chi$: transition factor, which is unity for monomolecular reactions; $k_B$: Boltzmann constant; $h$: Plank constant, and $T_p$ is the peak temperature of the DTA curve. The change of the entropy may be calculated according to the formula:

$$\Delta S^{\#} = R \ln\left(\frac{Ah}{e\chi k_B T_p}\right) \quad (8)$$

Since

$$\Delta H^{\#} = E^{\#} - RT_p, \quad (9)$$

when $E^{\#}$ is the average activation energy $E_a$ of the Achar and the Li–Tang methods (Table 3). The changes of the enthalpy $\Delta H^{\#}$ and Gibbs free energy $\Delta G^{\#}$ for the activated complex formation from the reagent can be calculated using the well known thermodynamic equation:

$$\Delta G^{\#} = \Delta H^{\#} - T_p \Delta S^{\#} \quad (10)$$

The enthalpy of activation ($\Delta H^{\#}$), entropy of activation ($\Delta S^{\#}$), free energy of activation decomposition ($\Delta G^{\#}$) were calculated at $T = T_p$ ($T_p$ is the DTA peak temperature at the corresponding stage in four heating rates), since this temperature characterizes the process, which is its most important parameter.

The calculated values of $\Delta H^{\#}$, $\Delta S^{\#}$ and $\Delta G^{\#}$ for the dehydration step of $AlPO_4 \cdot H_2O$ are summarized in Table 3. It was seen that the thermodynamic values calculated by the kinetic parameters from Achar method were close to the optimized values from Li–Tang method, and the respective correlation coefficients are preferable. The thermodynamic values of the dehydration of $AlPO_4 \cdot H_2O$ in this work are higher than those of synthetic $AlPO_4 \cdot 2H_2O$ (66.50 kJ $mol^{-1}$, −69.88 J $K^{-1}$ $mol^{-1}$ and 93.27 kJ $mol^{-1}$ for $\Delta H^{\#}$, $\Delta S^{\#}$ and $\Delta G^{\#}$, respectively) because the different methods and nature solid were applied. This indicates that the kinetic and thermodynamic functions of decomposition of each solid are dependent on process and the nature of non-isothermal method as well as TG. According to the kinetic data obtained from the TG curves, the dehydration step has negative entropy, which indicates that the complex is not spontaneously formed. In the terms of the activated complex theory (transition theory), a positive value of $\Delta S^{\#}$ indicates a malleable activated complex that leads to a large number of degrees of freedom of rotation and vibration [17, 18, 30–33] A result may be interpreted as a ''fast'' stage. On the other hand, a negative value of $\Delta S^{\#}$ indicates a highly ordered activated complex and the degrees of freedom of rotation as well as of vibration is less than they are in the non activated complex. The result may indicate a ''slow'' stage [17, 18]. On the basis of assumptions, the second step of the thermal decomposition of $AlPO_4 \cdot H_2O$ may be interpreted as ''slow'' stage. The negative entropy also indicates a more ordered activated state that should be possible through the dehydration process. The negative value of entropy of activation is compensated by the value of the enthalpy of activation, leading to almost the same value for the free energy of activation [17, 18]. The positive value of the enthalpy $\Delta H^{\#}$ is in good agreement with an endothermic effect in DTA data. The positive values of $\Delta H^{\#}$ and $\Delta G^{\#}$ for the dehydration stage shows that it is connected with the introduction of heat and is non-spontaneous process. These thermodynamic functions are in consistent with the results of kinetic parameters.

## Conclusions

$AlPO_4 \cdot H_2O$ decomposes in a single well-defined step by starting after 323 K and the final product is spherical particles $AlPO_4$. The dehydration of $AlPO_4 \cdot H_2O$ is important for its further treatments. The final product is confirmed by XRD data, scanning electron microscopy and FTIR measurements. The final product is confirmed by XRD, SEM and FTIR measurements. The kinetics and thermodynamics of the thermal dehydration of $AlPO_4 \cdot H_2O$ was studied using non-isothermal TG applying model-fitting method. The kinetics (E, A, model) and thermodynamics ($\Delta H^{\#}$, $\Delta S^{\#}$ and $\Delta G^{\#}$) parameters calculated for the dehydration reaction of $AlPO_4 \cdot H_2O$ by different methods and techniques were found to be consistent. This indicates that the activation energy of dehydration is independent on process and the nature of non-isothermal methods as well as TGA. A correlation between the $T_p$ (DTA) and the wavenumber of activated complex assigned to the breaking bond is possible, which can be used for identification in each thermal transition step of the studied compound and will be an alternative method for the calculated wavenumbers of interesting materials. On the basis of correctly established values of the apparent activation energy, pre-exponential factor and the changes of entropy, enthalpy and Gibbs free energy, certain conclusions can be made concerning the mechanisms and characteristics of the process, which play an important role in theoretical study, application development and industrial production of a compound as a basis

of theoretical. Consequently, these data will be important for further studies of the studied compound and are applied to solve various scientific and practical problems involving the participation of solid phases.

**Acknowledgment** The authors would like to thank the Chemistry and Physics Departments, Khon Kaen University for providing research facilities. This work is financially supported by Thailand Research Fund (TRF) and the Commission on Higher Education (CHE): Research Grant for New Scholar (MRG5280073), Ministry of Science and Technology, Thailand.

## References

1. Arjona MA, Alario Franco MA. Kinetics of the thermal dehydration of variscite and specific surface area of the solid decomposition products. J Therm Anal Cal. 1973;5:319–28.
2. Stojakovic D, Rajic N, Sajic S, Logar NZ, Kaucic V. A kinetic study of the thermal degradation of 3-methylaminopropylamine inside $AlPO_4$-21. J Therm Anal Cal. 2007;87:337–43.
3. Lagno F, Demopoulos GP. Synthesis of hydrated aluminum phosphate, $AlPO_4{\cdot}1.5H_2O$ ($AlPO_4{-}H_3$), by controlled reactive crystallization in sulfate media. Ind Eng Chem Res. 2005;44: 8033–8.
4. Youssif MI, Mohamed FSh, Aziz MS. Chemical and physical properties of $Al_{1-x}Fe_xPO_4$ alloys: Part I. Thermal stability, magnetic properties and related electrical conductivity. Mater Chem Phys. 2004;83:250–254.
5. Guti′errez-Mora F, Goretta KC, Singh D, Routbort JL, Sambasivan S, Steiner KA, et al. High-temperature deformation of amorphous $AlPO_4$-based nano-composites. J Eur Ceram Soc. 2006;26:1179–83.
6. Mostafa MR, Ahmed FSh. Characterization and catalytic behaviour of $Co_3(PO_4)_2$-$AlPO_4$ catalysts. Adsorp Sci Technol. 1998;16:285–93.
7. Campelo JM, Jaraba M, Luna D, Luque R, Marinas JM, Romero AA, et al. Effect of phosphate precursor and organic additives on the structural and catalytic properties of amorphous mesoporous $AlPO_4$ materials. Mater Chem Mater. 2003;15:3352–64.
8. Boonchom B, Youngme S, Srithanratana T, Danvirutai C. Synthesis of $AlPO_4$ and kinetics of thermal decomposition of $AlPO_4{\cdot}H_2O$-$H_4$ precursor. J Therm Anal Cal. 2008;91:511–6.
9. Boonchom B, Danvirutai C. Kinetics and thermodynamics of thermal decomposition of synthetic $AlPO_4{\cdot}2H_2O$. J Therm Anal Cal (Accepted manuscript).
10. Friedman HL. Kinetics of thermal degradation of char-forming plastics from thermogravimetry. J Polym Sci C. 1963;6:183.
11. Flynn H, Wall LA. Quick direct method for the determination of activation energy from thermogravimetric data. J Therm Anal. 1983;27:95.
12. Ozawa TA. A new method of analyzing thermogravimetric data. Bull Chem Soc Jpn. 1965;38:1881–6.
13. Achar BNN, Bridley GW, Sharp JH. Kinetics and mechanism of dehydroxylation process.III. Applications and limitations of dynamic methods. Proc Int Clay Conf, Jerusalem. 1966;1:67–73.
14. Tang W, Liu Y, Zhang H, Wang C. New approximate formula for Arrhenius temperature integral. Thermaochim Acta. 2003;408: 39–43.
15. Scaccia S, Carewska M, Bartolomeo AD, Prosini PP. Thermoanalytical investigation of nanocrystalline iron (II) phosphate obtained by spontaneous precipitation from aqueous solutions. Thermochim Acta. 2003;397:135–41.
16. Gabal MA, El-Bellihi AA, Ata-Allah SS. Effect of calcination temperature on Co(II) oxalate dihydrate−iron(II) oxalate dihydrate mixture DTA− TG, XRD, Mössbauer, FT-IR and SEM studies (Part II). Mater Chem Physics. 2003;81:84–92.
17. Vlaev L, Nedelchev N, Gyurova K, Zagorcheva M. A comparative study of non-isothermal kinetics of decomposition of calcium oxalate monohydrate. J Anal Appl Pyrolysis. 2008;81:253–62.
18. Vlase T, Vlase G, Doca M, Doca N. Specificity of decomposition of solids in non-isothermal conditions. J Therm Anal Cal. 2003; 72:597–604.
19. Rokita M, Handke M, Mozgawa W. Spectroscopic studies of polymorphs of $AlPO_4$ and $SiO_2$. J Mol Struct. 1998;450:213–7.
20. Müller G, Bódis J, Eder-Mirth G, Kornatowski J, Lercher JA. In situ FT-IR microscopic investigation of metal substituted $AlPO_4$-5 single crystals. J Mol Struct. 1997;410–411:173–8.
21. Colthup NB, Daly LH, Wiberley SE. Introduction to infrared and Raman spectroscopy. New York: Academic Press; 1964.
22. Vlaev LT, Nikolova MM, Gospodinov GG. Non-isothermal kinetics of dehydration of some selenite hexahydrates. J Solid State Chem. 2004;177:2663–9.
23. Budrugeac P, Segal E. Applicability of the Kissinger equation in thermal analysis. J Therm Anal Cal. 2007;88:703–7.
24. Budrugeac P, Muşat V, Segal E. Non-isothermal kinetic study on the decomposition of Zn acetate-based sol-gel precursor Part II. The application of the IKP method. J Therm Anal Cal. 2007;88: 699–702.
25. Zhang K, Hong J, Cao G, Zhan D, Tao Y, Cong C. The kinetics of thermal dehydration of copper(II) acetate monohydrate in air. Thermochim Acta. 2005;437:145–9.
26. Hong J, Guo G, Zhang K. Kinetics and mechanism of non-isothermal dehydration of nickel acetate tetrahydrate in air. J Anal Appl Pyrolysis. 2006;2:111–5.
27. Gao X, Dollimore D. The thermal decomposition of oxalates. Part 26: a kinetic study of the thermal decomposition of manganese (II) oxalate dihydrate. Thermochim Acta. 1993;215:47–63.
28. Gabal MA. Kinetics of the thermal decomposition of $CuC_2O_4$–$ZnC_2O_4$ mixture in air. Thermochim Acta. 2003;402:199–208.
29. Boonchom B, Danvirutai C. Thermal decomposition kinetics of $FePO_4{\cdot}3H_2O$ precursor to synthetize spherical nanoparticles $FePO_4$. Ind Eng Chem Res. 2007;46:9071–6.
30. J. Ŝesták. Thermodynamical properties of solids. Academia Prague; 1984.
31. Cordes HM. Preexponential factors for solid-state thermal decomposition. J Phys Chem. 1968;72:2185–9.
32. Criado JM, Pérez-Maqueda LA, Sánchez-Jiménez PE. Dependence of the preexponential factor on temperature. J Therm Anal Cal. 2005;82:671–5.
33. Boonchom B. Kinetics and thermodynamic properties of the thermal decomposition of manganese dihydrogenphosphate dihydrate. J Chem Eng Data. 2008;53:1553–8.